

## THERMAL BREAKAGE OF DOUBLE-PANE GLAZING BY FIRE

**Bernard R. Cuzzillo**  
Berkeley Engineering and Research, Inc.  
2216 Fifth Street  
Berkeley, CA 94710-2217

**Patrick J. Pagni**  
Mechanical Engineering Department  
University of California at Berkeley  
Berkeley, CA 94720-1740

### ABSTRACT

A model for double-pane window breakage due to heating by fire is developed that applies to both compartment fires and to urban/wildland intermix fires. This work builds on the model and computer code, BREAK1, for single-pane window breaking by fires, as described in previous publications, with additional features including the inter-pane gap heat transfer and sequential pane-breaking. A Mathcad-based computer code, McBreak, is developed that implements the double-pane model. Radiation is shown to dominate the inter-pane gap transport unless low-emissivity interior glass surfaces are used. Fires on the outdoor side of double-paned windows are included, since windows represent one of the most vulnerable features of dwellings in the urban/wildland intermix and double-paned windows help fire-harden a structure. Examples are presented for double-pane window breakage in compartment fires and wildland fires. Confirmed is the empirical observation that double-pane equipped structures might survive urban/wildland intermix fires better than their single-pane equipped neighbors.

### INTRODUCTION

Windows can be important dynamic components influencing fire behavior because when they break, they change from impermeable barriers to large ventilation sources.<sup>1,2</sup> Further, typical breakage events occur at critical stages of fire growth, and the resulting sudden venting can materially alter the course of a fire—possibly resulting in backdrafts or flashover. Thus, accurate prediction of glass breakage is critical to fire modeling. In the context of the urban/wildland intermix, windows can be a point of entry for wildfire conflagrations. Observation of fire damage patterns in the 20 October 1991 Oakland Hills Fire suggest that dwellings with double-paned windows at the periphery of the fire survived while their single-paned neighbors did not.<sup>3,4</sup>

Thermal stress causes glass breakage.<sup>5-11</sup> In this paper we consider the simplest and most common geometry in which the temperature in the central area of the glass pane rises much faster than that in the protected frame-covered area. There-

fore, the center expands more than the cool, frame-protected boundary. This puts the area under the frame in tension and causes early fracture because glass is brittle and its strength in tension is limited by imperfections on the edges. The glass breaks when the mean temperature,  $T_m$ , of the central pane reaches the break temperature,

$$T_m - T_i = fT_c, \quad (1)$$

where  $f = 2[\tanh(s/L) + \ln(\cosh(H/L)/\cosh(s/L))]L/(s+H)]^{-1}$  is a factor close to unity that accounts for the small amount of compression in the central heated panes and  $T_c = \sigma_g/E\beta$  is the characteristic temperature. These results have been verified experimentally.<sup>8,12-14</sup> Equations (4) and (44) of Ref. [15] should be replaced with the more exact Eq. (1) above which was also given previously as Eqs. 40 and 41 of Ref. [6].

The mean temperature is approximated in terms of the surface temperatures as

$$\theta_m = \chi(\theta(0,\tau) + \theta(1,\tau)) \quad (2)$$

where  $\tau = \alpha t/L^2$  and  $\theta = (T - T_i)/T_c$ .  $\chi = 0.5 \operatorname{erf}(\tau^{1/2})$  is a factor that accounts for the difference between the average of the two surface temperatures and the true mean temperature. Further details may be found in Refs. [6,7,8]. For a more general review of the glass-breaking-in-fires literature, see Ref. [16].

Joshi and Pagni<sup>6,7,8</sup> verified that for common windows and typical fires, the heat-transfer problem can be well approximated as one dimensional, through the thickness of the glass. The necessary conditions for this simplification are expressed in two dimensionless groups. First, the window frames must have an adequate shading width,  $s$ , compared to the thickness of the glass,  $L$ , such that  $s/L \geq 2$ . Second, the fire must be sufficiently fast compared to the transverse Fourier time, i.e.  $\alpha t/s^2 \leq 1$ . Under these conditions, the edge of the shaded glass under the frame remains close to its initial temperature. A typical value of  $s^2/\alpha$  is 625 seconds for a shading width of 15 mm. Glass breakage usually occurs in the first 10 minutes of a fire.

This paper reports the following extension of the previous work: the glass breaking analyses are extended to double-pane windows (see Fig. 1) with additional modeling of the inter-pane convective and radiative heat transfer; heat transfer coefficients and other parameters may be modeled as functions of time or temperatures; the previous Fortran numerical solution code, called

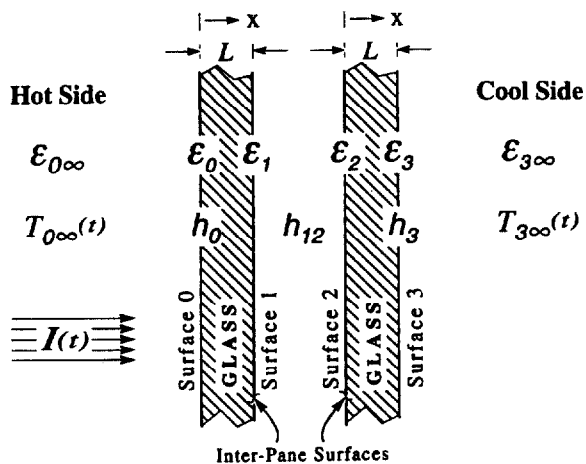


Figure 1. Double-Pane Geometry Showing the Numbering System and the Inter-Pane Gap.

BREAK1,<sup>17</sup> has been reimplemented in Mathcad,<sup>18</sup> a palimpsest-metaphor computing environment. The Mathcad version of BREAK1 is called McBreak. It is advantageous because of the ease with which time-dependent exposures, modifications, or enhancements are implemented. Also new here is an emphasis on fires attacking the structure from the outside rather than the compartment fire analyses previously reported.<sup>6,7,8</sup>

The double-pane extension is useful because multiple glazing layers are more common worldwide than single panes in modern structures, and their improved fire performance may play a significant role in protecting structures in the urban/wildland intermix.<sup>19</sup> Because the pane remote from the fire receives heat while its front-line neighbor is still intact, the second pane may not take as long to break. This effect is enhanced by the fact that the heating rates may be higher later in a compartment fire. On the other hand, under constant high-intensity exposure, the difference is not substantial. But in the general case of an arbitrarily specified exposure history, the time-to-break of the protected pane may not correlate at all to that of the fire-exposed pane.

For the benefit of readers unfamiliar with the glass breaking problem, a brief review of simple heating models is given. The double-pane heat transfer model is then presented with detailed prescriptions for the inter-pane transport. Finally, examples of double-pane window response to compartment fires and urban/wildland intermix fires are provided.

## HEAT TRANSFER ANALYSES FOR A SINGLE PANE

Before describing the double-pane problem, it is appropriate to review the single-pane problem in three stages:

1. *Lumped Mass, Linear Boundary Conditions:* The simplest model is a lumped, uniform glass temperature with  $h$ 's assumed constant. The governing equation and initial condition are

$$\frac{dT}{dt} = \frac{h_0}{\rho c L} (T_{\infty} - T) - \frac{h_1}{\rho c L} (T - T_{s1}), T(0) = T_i. \quad (3)$$

Introduce the dimensionless variables

$$\theta = \frac{T - T_f}{T_i - T_f} \quad \text{and} \quad \tau = \frac{h_0 + h_1}{\rho c L} t, \quad (4)$$

where

$$T_f = \frac{h_0 T_{\infty 0} + h_1 T_{\infty 1}}{h_0 + h_1}. \quad (5)$$

The solution is

$$\theta(\tau) = e^{-\tau}, \quad (6)$$

or

$$\frac{T(t) - T_f}{T_i - T_f} = \exp\left(-\frac{h_0 + h_1}{\rho c L} t\right). \quad (7)$$

The lumped model is inadequate for the fire application because the temperature gradient through the glass is an inherent part of the problem.<sup>9,10</sup> Conduction is primarily across the glass from a hot source to a cold sink.

*2. Distributed Mass, Linear Boundary Conditions, Internal Radiation Absorption:* In fire heat transfer, radiation often dominates. At the thermal wavelengths of interest,  $O(3\mu\text{m})$ , the glass is semi-transparent, and the fire's direct radiation may be absorbed through the thickness of the glass. The extinction length is typically 1 mm, while the glass thickness is typically 6 mm. Thus, the absorption of radiation is spatially relatively quick with 63% of the incident radiation deposited in the first sixth of the thickness. The wavelengths of radiation from the hot layer in a compartment fire are significantly longer than those from open flames and therefore occur in an opaque portion of the spectrum, so the hot-layer radiation is treated here as a boundary condition through  $h_r$ . The radiant flux through a semi-transparent medium is governed by Beer's law,

$$I(x) = I_0 e^{-x/l}. \quad (8)$$

The resulting heat source will be the derivative with respect to distance through the glass, so the new energy equation becomes

$$\rho c \frac{\partial T}{\partial t} = k \frac{\partial^2 T}{\partial x^2} + I(t) \frac{e^{-x/l}}{l}. \quad (9)$$

With the linearized boundary conditions

$$k \frac{\partial T(0,t)}{\partial x} = h_0(T(0,t) - T_{\infty 0}), \quad \text{and} \quad (10)$$

$$k \frac{\partial T(L,t)}{\partial x} = -h_1(T(L,t) - T_{\infty 1}),$$

and the initial condition,

$$T(x,0) = T_i, \quad (11)$$

these can be solved by conventional methods such as decomposition for constant  $I$  or variation of parameter for time-varying  $I(t)$ . In the decomposition method, the constant  $I$  solution is the sum of a steady-state temperature profile and a transient solution:

$$\theta(\xi, \tau) = u(\xi) + v(\xi, \tau), \quad (12)$$

where

$$\theta = \frac{T - T_i}{T_c - T_i}, \quad \xi = \frac{x}{L}, \quad \tau = \frac{\alpha t}{L^2} \quad \text{and} \quad T_c = \sigma_b / \epsilon \beta \quad (13)$$

from the breakage criterion. The steady-state is given by:

$$u(\xi) = -\gamma j e^{-\frac{\xi}{\gamma}} + A\xi + B \quad (14)$$

where

$$j = \frac{L}{k T_c} I, \quad A = Bi_0(-\xi j + B - \theta_{0\infty}) - j, \quad \gamma = \frac{l}{L} \quad (15)$$

and

$$B = \frac{-j e^{-\frac{1}{\gamma}} + j + Bi_0 \left( j \gamma e^{-\frac{1}{\gamma}} + j + \theta_{1\infty} \right) + Bi_1 Bi_0 (j \gamma + \theta_{0\infty})}{Bi_1 + Bi_0 + Bi_1 Bi_0}. \quad (16)$$

and the transient part,  $v(\xi, \tau)$ , is given by

$$v(\xi, \tau) = \sum_{n=0}^{\infty} b_n \phi_n(\xi) e^{-\lambda_n^2 \tau} \quad (17)$$

The eigenvalues are the roots of

$$\cot \lambda = \frac{\lambda^2 - Bi_1 Bi_0}{\lambda (Bi_1 + Bi_0)}, \quad (18)$$

and the eigenfunctions are given by

$$\phi_n(\xi) = Bi_0 \sin(\lambda_n \xi) + \lambda_n \cos(\lambda_n \xi), \quad (19)$$

and

$$b_n = \int_0^1 -u(\xi)\phi_n(\xi)d\xi / \int_0^1 \phi_n^2(\xi)d\xi \quad (20)$$

The variation of parameter solution, for the case of time-varying  $I(t)$ , can be found in Eqs. (20)–(28) of Ref. [7]. Both the decomposition and variation of parameter solutions were used to verify the McBreak numerical solutions. A simpler analytic solution, readily obtained by separation of variables, is the limit of no internal radiation absorption, i.e.  $I(t)$  or  $j(\tau) \rightarrow 0$ , and linearized radiation boundary conditions with the heat transfer coefficient as  $h = h_c + h_r$  with  $h_r = 4\mathcal{F}\sigma T_m^3$ , where  $T_m$  is a mean temperature and  $\mathcal{F}$  is a shape and surface property factor.

*3. Distributed Mass, Non-Linear Boundary Conditions, Radiation Absorption Through Thickness:* An analytical solution to the one- and two-dimensional, through-the-thickness, temperature profile with non-linear radiative boundary conditions and absorption has been developed.<sup>6,7,8</sup> A computer code, BREAK1, is available<sup>17</sup> that calculates the time to breakage for single panes based on the one-dimensional model. The governing equation and initial condition remain the same as in Eqs. (9) and (11). But now the boundary conditions become, at the fire side,  $x = 0$ :

$$-k \frac{\partial T(0,t)}{\partial x} = h_0(t)(T_{0\infty}(t) - T(0,t)) + \epsilon_{0\sigma} T_{0\infty}^4 - \epsilon_0 T^4(0,t) = q_0(t) \quad (21)$$

and at the cool side,  $x = L$ :

$$-k \frac{\partial T(L,t)}{\partial x} = h_1(t)(T(L,t) - T_{1\infty}(t)) + \epsilon_{1\sigma} T^4(L,t) - \epsilon_{1\infty} T_{1\infty}^4 = q_1(t), \quad (22)$$

where the new subscript convention is used uniformly here and in McBreak: surface 0 is hot and surface 1 is cool.

After non-dimensionalization, Laplace transformation, inversion only at the boundaries, and

further transformation<sup>7</sup> the final solutions at  $\xi = 0$  and 1 become:

On the fire-side surface of the glass,

$$\begin{aligned} \theta(0,\tau) = & 2 \int_0^{\sqrt{\tau}} u K_0(0,u) \phi_0(\tau - u^2) du \\ & + 2 \int_0^{\sqrt{\tau}} u K_1(0,u) \phi_1(\tau - u^2) du \\ & + \frac{2}{\gamma} \int_0^{\sqrt{\tau}} u K_r(0,u) j(\tau - u^2) du \end{aligned} \quad (23)$$

and on the cool-side surface,

$$\begin{aligned} \theta(1,\tau) = & 2 \int_0^{\sqrt{\tau}} u K_0(1,u) \phi_0(\tau - u^2) du \\ & + 2 \int_0^{\sqrt{\tau}} u K_1(1,u) \phi_1(\tau - u^2) du \\ & + \frac{2}{\gamma} \int_0^{\sqrt{\tau}} u K_r(1,u) j(\tau - u^2) du \end{aligned} \quad (24)$$

where  $u$  is a dummy variable,  $\xi$ , and  $\tau$  are given by Eq. (13), and  $j$  is given by Eq. (15). The kernels,  $K_0$ ,  $K_1$ , and  $K_r$ , given in Eqs. (12–19) of Ref. [7], are listed in the Appendix, as are the heat fluxes  $\phi_0$  and  $\phi_1$ . The most comprehensive model for surface temperature, given by Eqs. (23) and (24), are used here in the double-pane glazing breakage analyses. Use of the simpler models' results, Eqns. (7) or (12), could be substituted in a particular application where the appropriate assumptions were justified.

The three integrals in each of Eqs. (23) and (24) represent the effects of heat conduction into the glass from the fire side, heat conduction out of the cool side, and radiation absorption exponentially distributed through the thickness of the glass. Each integral is a weighted integration of its respective heat flux. These solutions require numerical integration, which was previously implemented by BREAK1 in Fortran, and in the present case is done by McBreak in Mathcad. The new code was verified both by detailed comparison to BREAK1 using several identical input data sets and by comparison to analytic solutions for the case of linearized radiation boundary conditions.

## EXTENSION TO DOUBLE-PANE WINDOWS

Figure 1 shows the configuration of the double-pane problem in which the glass surfaces are numbered from fire side to cool side as 0,1,2,3. The boundary conditions for the single pane are transferred to the exterior surfaces (0 and 3) of the glazing system. There are now two coupled conduction heat-transfer problems, one for each pane. The coupling is expressed in terms of the boundary conditions for the two interior surfaces. The inter-pane heat transfer coefficient,  $h_{12}(T,t)$ , is taken as common to both surface 1 and 2, thus its subscript is "12." For surface 1, the temperature of what would be termed the "free stream" in an ordinary convection problem is the temperature of surface 2 for this problem. Likewise, the "free stream" temperature for surface 2 is the temperature of surface 1. Radiatively, grey infinite parallel plates are assumed, with the view factor between the two surfaces taken as unity, so that the net radiative resistance<sup>20</sup> is  $\epsilon_1^{-1} + \epsilon_2^{-1} - 1$ . Thus, the interior surfaces' boundary conditions are

$$\begin{aligned}
 -k \left. \frac{\partial T(L,t)}{\partial x} \right|_{\text{fire-side pane}} &= -q_1(t) \\
 &= q_2(t) \\
 &= -k \left. \frac{\partial T(0,t)}{\partial x} \right|_{\text{cool-side pane}}, \quad (25)
 \end{aligned}$$

where:

$$\begin{aligned}
 q_2(t) &= h_{12}(T,t)(T_1(t) - T_2(t)) \\
 &+ \left( \frac{1}{\epsilon_1} + \frac{1}{\epsilon_2} - 1 \right)^{-1} \sigma (T_1^4(t) - T_2^4(t)). \quad (26)
 \end{aligned}$$

$q_2(t) = -q_1(t)$  since the thermal storage capacity of the inter-pane gap is negligible. Note that the direct radiation flux,  $I(t)$ , reaching the cool pane is zero since the hot pane is assumed to block all of it. It is also assumed that the gap gas temperature rise prior to breakage is sufficiently small that the gap pressure rise can be neglected.

Until the hot pane breaks, all four surface temperatures are computed simultaneously, with the cool pane receiving heat from the hot pane and delivering heat to the cool-side ambient. This

thermal coupling of the two panes shortens the cool pane's time to breakage and is an important advantage of the double-pane model over the sequential use of the single-pane model. As soon as the hot pane breaks, the boundary conditions for surface 2, the interior surface of the cool pane, are assumed to switch to those formerly assigned to surface 0—namely the current fire convection and direct and indirect radiation. In this double-pane model, the pane remote from the fire is conservatively assumed to be subjected directly to the current fire conditions as soon as the fire-exposed pane breaks. Experimental evidence<sup>11</sup> suggests that in the absence of wind loading or significant interior overpressures, a cracked pane may remain in the frame for a substantial period. This glass fall-out problem remains to be solved.

For modeling urban/wildland fires, separate convective and radiative temperatures may be specified. In this case, the convective temperature can remain at ambient while a specific portion of the radiative field, incorporated via a configuration factor, achieves flame temperature. The rest of the radiative field may also stay close to ambient temperature.

## CONVECTIVE HEAT TRANSFER COEFFICIENTS

The three heat transfer coefficients are  $h_0(T,t)$ ,  $h_{12}(T,t)$ , and  $h_3(T,t)$ , representing the fire-side, the inter-pane air gap, and the cool side, respectively. As indicated, these may be functions of any temperature or of time. The one most likely to benefit from the enhanced dependence is on the fire side,  $h_0(T,t)$ , as conditions here may vary significantly during the course of exposure.

Considering no wind—natural convection only—Grashoff or Rayleigh number correlations<sup>21</sup> indicate that for most single-pane windows turbulent natural-convection will be present at surface 0. Corresponding heat transfer coefficients range from 3 to 8 W/m<sup>2</sup>K. For double-pane windows, before breakage of the hot pane, surface 3—the cool-pane exterior—will be minimally affected by the fire and therefore remain near the cool free-stream temperature. Therefore, during the pre-breakage phase, the flow on surface 3 will be nearly laminar because of the small temper-

ature difference, and the value of  $h_3$  will be  $\leq 3 \text{ W/m}^2\text{K}$ .<sup>21</sup> This means that radiation heat transfer may dominate even on this cool surface. Under wildland fire conditions or inside most compartments, however, forced convection will be more likely than natural convection due to the high winds or rapid circulation. Values of the convective coefficient range under these conditions range from  $12 \text{ W/m}^2\text{K}$  at a wind speed of  $2 \text{ m/s}$  ( $4.5 \text{ mph}$ ) to  $50 \text{ W/m}^2\text{K}$  at  $20 \text{ m/s}$  ( $45 \text{ mph}$ ) based on a widely used correlation.<sup>22,23</sup>

In the inter-pane air gap, a standard Rayleigh number correlation<sup>24</sup> based on the gap distance,

$$Nu = [1 + (0.0303Ra^{0.402})^{11}]^{1/11} \quad (27)$$

shows that conduction through stagnant air is the dominant transport mechanism for gaps  $\leq 10\text{mm}$ .  $h_{12}$  reaches a minimum of  $2.4 \text{ W/m}^2\text{K}$  in air at a gap of between  $12 \text{ mm}$  and  $16 \text{ mm}$  before convective movement of air begins to drive it higher as shown in Fig. 2. Typical double-pane windows are designed to take advantage of this minimum. Radiation heat transfer through the gap depends strongly on the emissivity of the glass or its interior coatings. Figure 3 shows the linearized radiation heat transfer coefficient

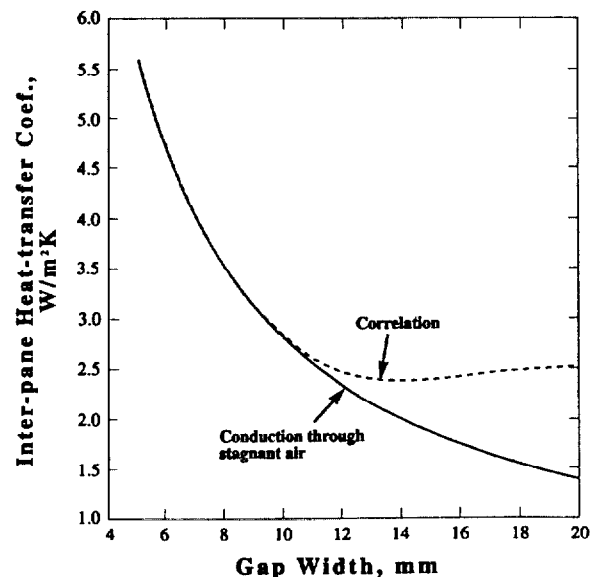


Figure 2. Inter-Pane Heat-Transfer Coefficient,  $h_{12}$ , with the Inter-Pane Gas as Air at  $325\text{K}$  and  $T_1 - T_2 = 50\text{K}$ . The solid line is stagnant conduction and the dashed line the Rayleigh no. correlation,<sup>22</sup>  $Nu[1 + (0.0303Ra^{0.402})^{11}]^{1/11}$ . For argon as the gap gas, lower  $h$  by a factor of approximately  $\frac{2}{3}$ .

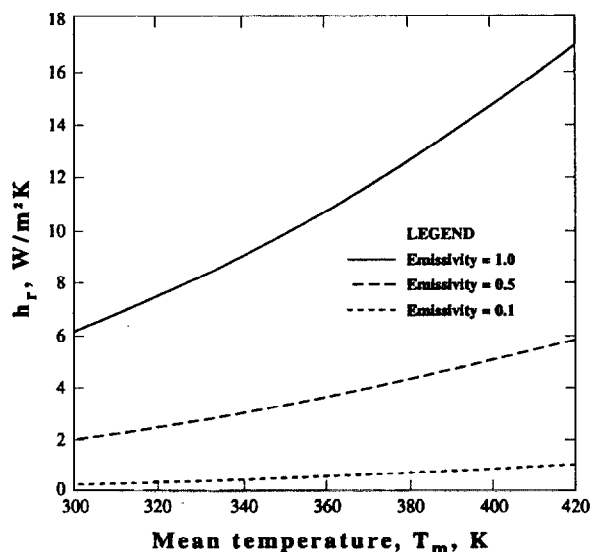


Figure 3. Linearized Heat-Transfer Coefficient,  $h_r$ , as a Function of Mean Temperature,  $T_m$ , where

$$h_r \approx 4\sigma T_m^3 \left( \frac{1}{\epsilon_1} + \frac{1}{\epsilon_2} - 1 \right)^{-1}, \text{ and } \epsilon_1 = \epsilon_2.$$

with both interior surfaces at emissivities of  $\epsilon = 1.0, 0.5$ , and  $0.1$ . At unity emissivity, radiation dominates convection. However, commercially available<sup>19</sup> windows have “low-e” coatings with emissivities as low as  $0.04$ . Assuming the emissivity remains low in the near infrared,  $h_r$  becomes less than  $h_c$ , as shown by comparing Figs. 2 and 3. Uncoated glass typically has an emissivity from  $0.8$  to  $0.9$ .

## RESULTS

As an example of applying the double-pane model to compartment fires, consider the default case given in Ref. [17] describing an exponentially growing fire in a standard compartment. The input parameters are given in Fig. 4, which shows the temperature histories of the four surfaces as light dashed lines. The heavy solid line is the hot layer temperature predicted by a typical compartment fire by FIRST.<sup>25</sup> The first pane breaks at  $134 \text{ s}$  and then the direct heating of the second pane begins, as shown by the steep increase in the surface 2 temperature. The mean temperature of the second pane has only risen  $5 \text{ K}$  at  $134 \text{ s}$ . The second pane breaks at  $203 \text{ s}$  when its mean temperature reaches the breakage threshold, Eqs. (1-2). Figure 5 shows the same case but without direct radiation, i.e.  $I = 0$ .

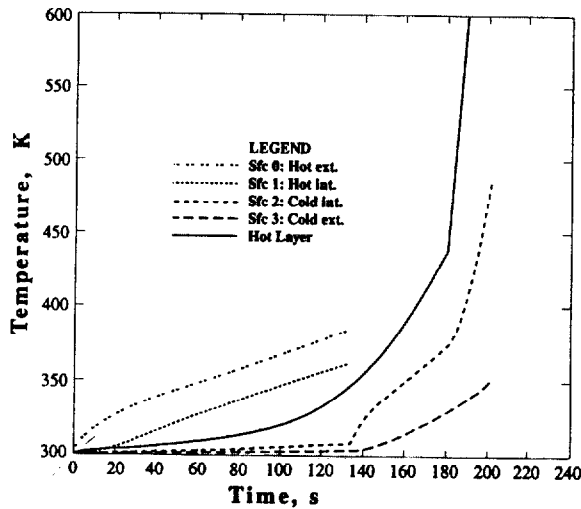


Figure 4. McBreak Double-Pane Results Using Default BREAK1 Input Data:  $E=7 \times 10^{10} \text{ Pa}$ ,  $\beta=9.5 \times 10^{-6} \text{ K}^{-1}$ ,  $\sigma_{ultimate \ tensile}=4.7 \times 10^7 \text{ Pa}$ ,  $l=1.0 \text{ mm}$ ,  $k=0.76 \text{ W/mK}$ ,  $\alpha=3.6 \times 10^{-7} \text{ m}^2/\text{s}$ ,  $L=6.4 \text{ mm}$ ,  $s=15 \text{ mm}$ ,  $H=0.5 \text{ m}$ ,  $h_0=50 \text{ W/m}^2\text{K}$ ,  $h_{12}=h_3=10 \text{ W/m}^2\text{K}$ ,  $T_{0,a}(t)$  as shown,  $T_{3,a}=T_i=300\text{K}$ ,  $l(t)=10 \text{ kW/m}^2$ , and unity emissivities.

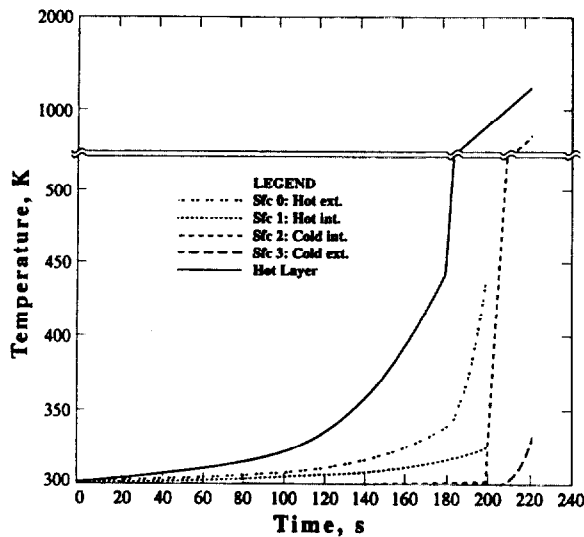


Figure 5. McBreak Double-Pane Results Using Default BREAK1 Input Data Values. All input parameters are the same as in Figure 4 except  $l(t)=0$ .

In a realistic wild-fire context, a bush or tree some distance from the window may be ignited by an air-born brand.<sup>3</sup> For typical vegetation, this heat source will have a short duration before burnout. If the second pane can extend the life of the window beyond vegetative burnout, the structure will not ignite. Figures 6a,b and c explore this problem for a fire that has a constant heat-release rate that lasts 6 minutes. Figure 6a shows the response of a double pane window to

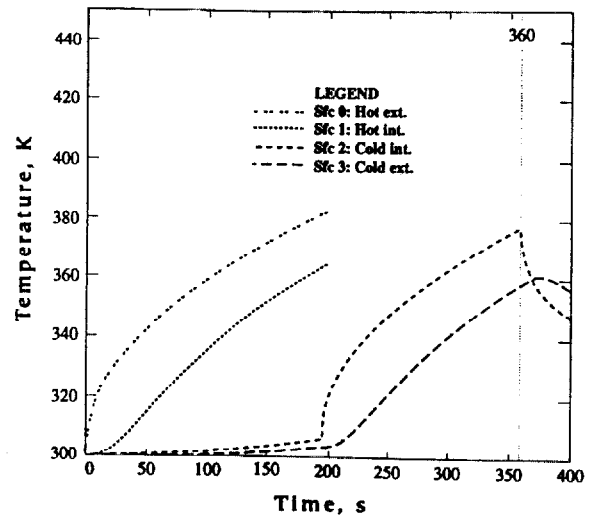


Figure 6a. Urban/Wildland Intermix Application of Double-Pane Window Glass Breakage. Outer pane is exposed to burning vegetation at 1000K for 360s. Exterior radiative heating with  $\mathcal{F}=0.15$  occurs with simultaneous convective and radiative ( $\mathcal{F}=0.85$ ) cooling at 300K. All other input parameters are the same as in Fig. 5 except  $h_0=50 \text{ watts/m}^2\text{K}$ ,  $h_{12}=2.5 \text{ watts/m}^2\text{K}$ , and  $h_3=3 \text{ watts/m}^2\text{K}$ . The cool pane does not break.

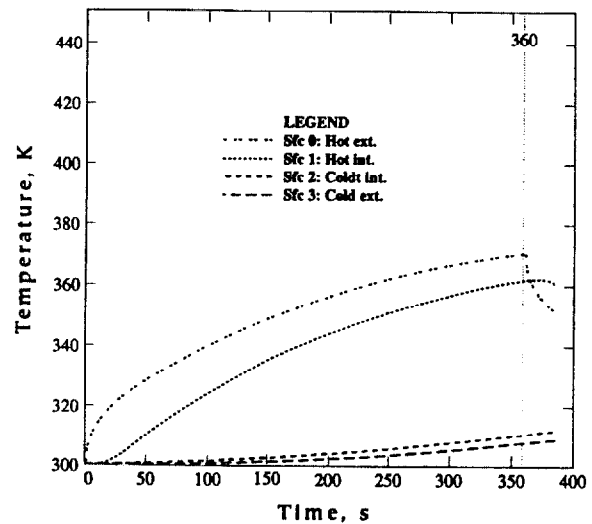


Figure 6b. Same Problem as Fig. 6a But With  $\mathcal{F}=0.10$ . Neither pane breaks.

a burning bush which is modeled as a black circular disk at 1000 K that takes up 15% of the window's view factor on the hot side. This 15% is determined, e.g., from the view-factor formula  $\mathcal{F}_{d1-2}=r^2/(h^2+r^2)$  where  $h$  is the distance from the window.<sup>20</sup> This 15% view factor implies a one-meter radius fire at 2.4-meters away, aligned with the window, which represents an initial incident flux of 8.44 kW/m<sup>2</sup>. The remaining 85%

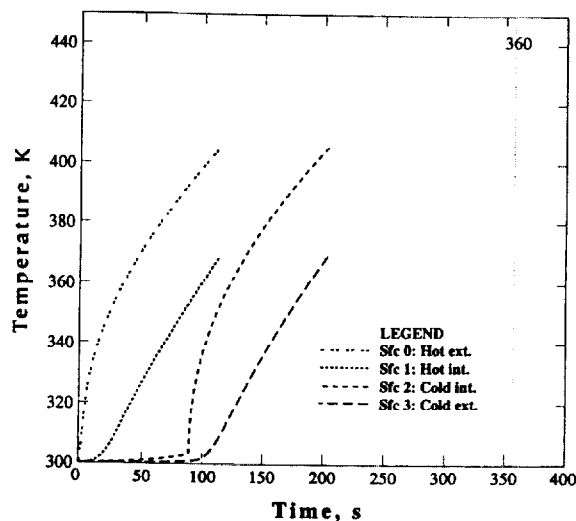


Figure 6c. Same Problem as Fig. 6a But With  $\mathcal{F}=0.25$ . Both panes break.

of the radiative view and the convective temperature are at an ambient of 300 K. The pane nearer the source breaks in about  $3\frac{1}{2}$  minutes. The remaining pane's temperature then begins to climb, but the source burns out and the cool pane and the structure survive. Figures 6b and 6c show similar situations with smaller and larger view factors (0.10 with  $5.62 \text{ kW/m}^2$  and 0.25 with  $14.1 \text{ kW/m}^2$ ) so that neither or both panes break, respectively.

These results suggest that the standard clearance distance of 30 m for structures in the urban/wildland intermix might be lowered for structures with double-pane windows. Further, if surface 1 is low-emissivity coated, the window will have greatly enhanced wildfire resistance. This could be practical since this is an interior surface which will stay clean and undamaged for years and thus maintain its low emissivity.

## CONCLUSIONS

A double-pane window breakage model is described that calculates the temperature histories of all four glass surfaces with quantification of the inter-pane gap heat transport mechanisms. Practical example results are given in the limit where all incident radiation is absorbed by the first pane. Variations in fire radiation characteristics, glass optical properties, and glass thickness are important to the assumption that the first pane is opaque. The radiation decay length,

which is approximated here as a constant, is in fact a function of wavelength so that higher temperature sources may violate the opacity assumption.

These calculations show relatively little temperature rise in the second pane before the first pane is both broken and removed. While it is not appropriate to assume that a double-pane window will take twice as long as a single-pane window to break, sequential use of a single pane model, e.g. BREAK1, may suffice in many applications. A major difficulty is that both McBreak and BREAK1 predict only the initial cracking time, not the time when the pane actually falls out. Pane removal is a critical problem which remains to be solved for both single and double paned systems. It may depend on the pressure history in the compartment as well as the pane mounting details. In an exponentially growing compartment fire, once the first pane is removed, the exposed second pane may last only a few seconds since the hot layer temperature is now so high. The wildland fire scenario is different in that vegetation burns intensely but is rapidly consumed. The heating of the second pane is minimal before breakage of the exterior hot pane, and the primarily radiative heating will be delayed until removal of the first pane. The cool second pane may provide just the extra time needed for the window to survive the short-duration burst of radiation from vegetative burning, preventing fire penetration into the structure.

Two important areas of future work are: Comparisons with double-pane glazing breakage experiments and the development of new inter-gap films with fire resistive properties. An extensive series of double-pane window experiments are underway at the University of Ulster.<sup>26</sup> Comparisons will be made when these results become available. This study has identified a potentially significant role for inter-pane films as fire protection tools. If energy-efficient films, that were also heat resistant, were adhered to both interior surfaces, the film could hold the broken first pane in place, shielding the second pane and substantially extending the window lifetime. This important application requires further exploration.

## ACKNOWLEDGMENTS

This work was partially supported by grant 60NANB80848 from the Building and Fire

Research Laboratory of the National Institute of Standards and Technology, U.S.D.O.C. The authors also gratefully acknowledge Berkeley Engineering and Research, Inc. for its support of this project.

## NOMENCLATURE

$Bi$	Biot number, $hL/k$
$c$	Specific heat
$E$	Young's modulus
$\mathcal{F}$	Radiative shape, view, or configuration factor
$f$	Geometric stress factor
$H$	Half-width of window
$h$	Heat transfer coefficient
$I(t)$	Prescribed dimensional radiant heat flux
$j(t)$	Dimensionless $I(t)$ , $I(t)L/kT_c$
$K$	Kernels
$k$	Thermal conductivity
$L$	Glass thickness
$l$	Radiation decay length
$Nu$	Nusselt number, $hL/k$
$q$	Dimensional heat flux
$Ra$	Rayleigh number, $Ra_d = \frac{g\beta(T_s - T_\infty)d^3}{\nu\alpha}$ , where $g$ the acceleration of gravity, $\beta$ is the coefficient of thermal expansion, $T_s$ is the surface temperature, $T_\infty$ is the free-stream temperature, and $d$ is the inter-pane gap distance.
$s$	Shading width
$T$	Temperature
$t$	Time
$x$	Distance through the thickness of the glass

## Greek

$\alpha$	Thermal diffusivity
$\beta$	Thermal expansion coefficient
$\gamma$	Dimensionless decay length, $l/L$
$\epsilon$	Emissivity
$\phi$	Heat flux at the surface of the glass
$\rho$	Mass density
$\theta$	Dimensionless temperature, $(T - T_i)/T_c$ or $(T - T_p)/(T_i - T_p)$
$\sigma$	Stefan-Boltzmann constant, $5.67 \times 10^{-8} \text{W/m}^2\text{K}^4$ , or stress
$\tau$	Dimensionless or Fourier time, $\alpha t/L^2$
$\chi$	Transient conversion function

$\xi$  Dimensionless coordinate through glass thickness,  $x/L$

## Subscripts

0	Hot-side pane, exterior surface
1	Hot-side pane, interior surface
2	Cool-side pane, interior surface
3	Cool-side pane, exterior surface
$b$	Breakage
$c$	Characteristic, as in the temperature rise for glass breakage, $T_c$ , or Convective, as in $h_c$ .
$i$	Initial value
$r$	Radiative
$m$	Mean
$\infty$	ambient

## REFERENCES

- Emmons, H.W., "The Needed Fire Science," *Fire Safety Science – Proceedings of the First International Symposium*, eds. C.E. Grant and P.J. Pagni, pp. 33-53, Hemisphere, Washington, D.C., 1986.
- Pagni, P.J., "Fire Physics – Promises, Problems and Progress," *Fire Safety Science – Proceedings of the Second International Symposium*, eds. T. Wakamastu, et al. pp. 49-66, Hemisphere, Washington, D.C., 1988.
- Pagni, P.J., "Causes of the 20 October 1991 Oakland Hills Conflagration," *Fire Safety Journal*, Vol. 21, pp. 331-339, 1993.
- Kluver, M., "Observations from the Oakland Hills Fire," *Building Standards*, Vol. 61, pp. 4-9, 1992.
- Seidel, H. and Kiefer, W., "Stand der Entwicklung von Feuerwiderstandsfähigen Verglasungen nach DIN 4102" (State of Development of Fire Resistant Glazing According to German Standard DIN 4102), *Glastechnische Berichte*, Vol. 51, pp. 111-124, 1978.
- Pagni, P.J. and Joshi, A.A., "Glass Breakage in Fires," *Fire Safety Science – Proceedings of the Third Intermediate Symposium* eds.

- G. Cox and B. Langford, pp. 791-802, Elsevier, London, U.K. 1991.
7. Joshi, A.A. and Pagni, P.J., "Fire Induced Thermal Fields in Window Glass I—Theory," *Fire Safety Journal*, Vol. 22, pp. 25-43, 1994.
  8. Joshi, A.A. and Pagni, P.J., "Fire-Induced Thermal Fields in Window Glass II—Experiments," *Fire Safety Journal*, Vol. 22, pp. 45-65, 1994.
  9. Keski-Rahkonen, O., "Breaking of Window Glass Close to Fire," *Fire and Materials*, Vol. 12, pp. 61-69, 1988.
  10. Keski-Rahkonen, O., "Breaking of Window Glass Close to Fire, II: Circular Panes," *Fire and Materials*, Vol. 15, pp. 11-16, 1991.
  11. McArthur, N.A., "The Performance of Aluminum Building Products In Bushfires," *Fire and Materials*, Vol. 15, pp. 117-125, 1991.
  12. Skelly, M.J., Roby, R.J. and Beyler, C.L., "Experimental Investigation of Glass Breakage in Compartment Fires," *Journal of Fire Protection Engineering*, Vol. 3, pp. 25-34, 1991.
  13. Hassani, S.K.S., Shields, T.J. and Silcock, G.W., "An Experimental Investigation into the Behavior of Glazing in Enclosure Fire," *Journal of Applied Fire Science*, Vol. 4, pp. 303-323, 1995.
  14. Mongia, L.M. and Pagni, P.J., "Experimental Comparisons with BREAK1," Progress report for NIST-BFRL Grant No. 60NANB3D1438, 1997.
  15. Sincaglia, P.E. and Barnett, J.R., "Development of a Glass Window Fracture Model for Zone-Type Computer Fire Codes," *Journal of Fire Protection Engineering*, Vol. 8, pp. 101-118, 1997.
  16. Hassani, S.K.S., Shields, T.J., and Silcock, G.W., "Thermal Fracture of Window Glazing: Performance of Glazing in Fire," *Journal of Applied Fire Science*, Vol. 4, pp. 249-263, 1995.
  17. Joshi, A.A. and Pagni, P.J., *Users' Guide to BREAK1, The Berkeley Algorithm for Breaking Window Glass in a Compartment Fire*, National Institute of Standards and Technology Report No. NIST-GCR-91-596, Gaithersburg, MD, 1991.
  18. MathSoft Inc., *Mathcad 7 Professional, Users' Guide*, MathSoft Inc., Cambridge, MA, 1997.
  19. Fissette, P., "High-Performance Glazing," *Fine Homebuilding*, Vol. 55, pp. 78-82, 1989.
  20. Siegel, R. and Howell, John R., *Thermal Radiation Heat Transfer*, Second Edition, McGraw-Hill, New York, 1981, p. 240 and Appendix C.
  21. Atreya, A., "Convection Heat Transfer," in *Handbook of Fire Protection Engineering*, 2nd Edition, DiNenno, P.J., et al., eds., National Fire Protection Association, Quincy, MA, 1988, Table 1-3.4, pp. 1-60.
  22. Arasteh, D.K., et al, "A Versatile Procedure for Calculating Heat Transfer through Windows," *ASHRAE Transactions*, Vol. 95, pp. 755-765, 1989, Equation 38b.
  23. Ito, N. and Kimura, K., "A Field Experiment Study on the Convective Heat Transfer Coefficient on the Exterior Surface of a Building," *ASHRAE Transactions*, Vol. 78, pp. 184-191, 1972.
  24. Elsherbiny, S.M., Raithby, G.D., and Hollands, K.G.T., "Heat Transfer by Natural Convection Across Vertical and Inclined Air Layers," *Transactions of the ASME, Journal of Heat Transfer*, Vol. 104, pp. 96-102, 1982. Equation (A4).
  25. Mitler, H.E., and Rockett, J.A., "Users' Guide to FIRST, A Comprehensive Single-Room Fire Model," NBSIR 87-3595, NBS, Washington, 1987.
  26. Shields, T.J., Private Communication, 1997.

## APPENDIX

The heat fluxes are given by

$$\phi_0(t) = A + B\theta(0,\tau) + C_0\theta^2(0,\tau) + D_0\theta^3(0,\tau) + E_0\theta^4(0,\tau)$$

and

$$\phi_1(t) = F + G\theta(1,\tau) - C_1\theta^2(1,\tau) - D_1\theta^3(1,\tau) - E_1\theta^4(1,\tau)$$

where

$$A = \frac{h_2 L (T_{0\infty}(t) - T_i) + \epsilon_{\infty} \sigma L T_{0\infty}^4(t) - \epsilon_0 \sigma L T_i^4}{k T_c},$$

$$B = -\frac{h_0 L + 4\epsilon_0 \sigma T_i^3 L}{k},$$

$$C_n = -\frac{6\epsilon_n T_c T_i^2 L}{k},$$

$$D_n = -\frac{4\epsilon_n \sigma T_c^2 T_i L}{k},$$

$$E_n = -\frac{\epsilon_n \sigma T_c^3 L}{k},$$

$$F = \frac{h_1 L (T_i - T_{1\infty}(t)) - \epsilon_{\infty} \sigma T_{1\infty}^4(t) L + \epsilon_1 \sigma L T_i^4}{k T_c},$$

and  $G = \frac{h_1 L + 4\epsilon_1 \sigma T_i^3 L}{k}.$

The kernels are given by the following set of Mathcad expressions. Conditionals within parentheses evaluate to one if true and zero if false.

$$n = 1 .. 10$$

$$f_{il}(\xi, \tau) = -\left[1 + 2 \cdot \left[\sum_n (-1)^{n(\xi < 1)} \cdot \exp(-n^2 \cdot \pi^2 \cdot \tau)\right]\right]$$

$$f_{ol}(\xi, \tau) = 1 + 2 \cdot \left[\sum_n (-1)^{n(\xi > 0)} \cdot \exp(-n^2 \cdot \pi^2 \cdot \tau)\right]$$

$$f_{radl}(\xi, \tau) =$$

$$\exp\left(\frac{-1}{\gamma}\right) \cdot \left[-\gamma + \frac{2}{\gamma} \cdot \sum_n \frac{(-1)^{n(\xi < 1)}}{-n^2 \cdot \pi^2 - \frac{1}{\gamma^2}} \cdot \exp(-n^2 \cdot \pi^2 \cdot \tau)\right] \dots$$

$$+ (-1) \cdot \left[-\gamma + \frac{2}{\gamma} \cdot \sum_n \frac{(-1)^{n(\xi > 0)}}{-n^2 \cdot \pi^2 - \frac{1}{\gamma^2}} \cdot \exp(-n^2 \cdot \pi^2 \cdot \tau)\right]$$

$$K_i(\xi, u) = (u \cdot (u > .1) + .1 \cdot (u \leq .1)) \cdot f_{il}[\xi, u^2 \cdot (u > .1) + .1^2 \cdot (u \leq .1)]$$

$$K_o(\xi, u) = (u \cdot (u > .1) + .1 \cdot (u \leq .1)) \cdot f_{ol}[\xi, u^2 \cdot (u > .1) + .1^2 \cdot (u \leq .1)]$$

$$K_r(\xi, u) = u \cdot f_{radl}(\xi, u^2)$$